RESEARCH ARTICLE

The degenerative impact of hyperglycemia on the structure and mechanics of developing murine intervertebral discs

Marianne Lintz[1] | Remy E. Walk[2] | Simon Y. Tang[2,3,4] | Lawrence J. Bonassar[1,5]

[1]Meinig School of Biomedical Engineering, Cornell University, Ithaca, New York, USA

[2]Department of Biomedical Engineering, Washington University in St. Louis, St. Louis, Missouri, USA

[3]Department of Mechanical Engineering and Materials Science, Washington University in St. Louis, St. Louis, Missouri, USA

[4]Department of Orthopaedic Surgery, Washington University in St. Louis, St. Louis, Missouri, USA

[5]Sibley School of Mechanical and Aerospace Engineering, Cornell University, Ithaca, New York, USA

Correspondence
Lawrence J. Bonassar, Meinig School of Biomedical Engineering, Sibley School of Mechanical and Aerospace Engineering, 149 Weill Hall, Cornell University, Ithaca, NY 14853, USA.
Email: lb244@cornell.edu

Funding information
Colin MacDonald Fund; Daedalus Innovation Fund; National Institute of Health, Grant/Award Numbers: K01AR069116 (S. Y. T.), R01AR074441 (S. Y. T.), R01AR077678 (S. Y. T.), T32DK108742 (R. E. W.); New York State Advanced Research Fund

Abstract

Introduction: Diabetes has long been implicated as a major risk factor for intervertebral disc (IVD) degeneration, interfering with molecular signaling and matrix biochemistry, which ultimately aggravates the progression of the disease. Glucose content has been previously shown to influence structural and compositional changes in engineered discs in vitro, impeding fiber formation and mechanical stability.

Methods: In this study, we investigated the impact of diabetic hyperglycemia on young IVDs by assessing biochemical composition, collagen fiber architecture, and mechanical behavior of discs harvested from 3- to 4-month-old db/db mouse caudal spines.

Results: We found that discs taken from diabetic mice with elevated blood glucose levels demonstrated an increase in total glycosaminoglycan and collagen content, but comparable advanced glycation end products (AGE) levels to wild-type discs. Diabetic discs also contained ill-defined boundaries between the nucleus pulposus and annulus fibrosus, with the latter showing a disorganized and unaligned collagen fiber network at this same boundary.

Conclusions: These compositional and structural changes had a detrimental effect on function, as the diabetic discs were twice as stiff as their wild-type counterparts and demonstrated a significant resistance to deformation. These results indicate that diabetes may predispose the young disc to DDD later in life by altering patterns of extracellular matrix deposition, fiber formation, and motion segment mechanics independently of AGE accumulation.

KEYWORDS
annulus fibrosus, degenerative disc disease, diabetes, proteoglycans

1 | INTRODUCTION

Lower back pain is an extremely prevalent disorder and one of the leading causes of disability worldwide, with approximately 50% to 80% of the adult population experiencing symptoms at least once in their lifetime.[1,2] Although a variety of risk factors are attributed to its onset, degeneration of the intervertebral disc (IVD) is implicated as a major contributor to its advancement.[3–5] Disc degeneration is a complex, multifactorial process characterized by deterioration of the disc's composition and structure, as well as irreversible changes to

its endogenous cell population.[3-7] As the disease progresses the highly hydrated nucleus pulposus (NP) loses water content and is rendered unable to sustain loads, while the complex fiber network of the surrounding annulus fibrosus (AF) becomes increasingly disorganized, eventually leading to rupture or herniation of the disc. The accumulation of damage to the AF triggers a degenerative cascade, favoring catabolism and upregulating matrix metalloproteases (MMPs) and other factors contributing to extracellular matrix (ECM) degeneration,[8-14] which the cell population is no longer able to repair.

Diabetes is a collection of chronic metabolic illnesses with varying etiologies, but common symptoms characterized by improper production, and in some cases resistance, to the hormone insulin which in turn results in heightened blood glucose levels or hyperglycemia.[15-18] With time, diabetes and its associated symptoms result in additional comorbidities such as cardiovascular disease, loss of vision or total blindness, musculoskeletal disorders, nerve damage, impaired wound healing, and so forth, all of which can lead to decreased quality of life or even death.[16,18-22]

Diabetes is also a common comorbidity for degenerative disc disease.[23-33] Clinical studies have indicated that patients receiving surgical intervention for lumbar disc disease demonstrate a higher incidence of diabetes.[28-30] Additionally, diabetic patients have been found to be significantly more likely to receive surgical treatments for lumbar disc disease than nondiabetics, and while they experience higher initial benefit from surgery,[29] they are seven times more likely to require additional surgical intervention.[32] Laboratory studies meanwhile have attempted to elucidate the mechanisms under which diabetes contributes to DDD, finding strong evidence suggesting that diabetes has a degenerative effect on the disc and may interfere with molecular pathways associated with disc disease.[24,26,33-35] However, it can be difficult to discern which changes arise as a direct consequence of diabetes from those associated with typical degeneration, as both diseases are time-dependent and DDD is only diagnosed following reports of painful symptoms, and the damage is discovered once they are well established.

While the connections between diabetes and DDD have been reported clinically, the mechanism behind this connection is still not fully understood, particularly at the molecular level. Previous studies have investigated the effect of glucose on the formation of collagen fibers in fibrocartilaginous tissues, similar to the AF of the IVD.[36-38] High levels of glucose drove contractile forces and increased proteoglycan content, which ultimately had a negative effect on the formation of the collagen network. Fiber organization was maximal at low physiologic levels of glucose (500 mg/L), while the higher range of physiologic and superphysiological concentrations (4500 mg/L) resulted in the formation of unaligned and disorganized fiber networks. Utilizing self-assembling tissue engineered IVD (TE-IVD) constructs[39-44] to investigate the impact of glucose on the formation of the engineered disc, we showed that these superphysiological levels of glucose also had a detrimental effect on mechanics: TE-IVDs with elevated proteoglycan content and diminished fiber alignment in the AF region demonstrated lower equilibrium moduli when subjected to

mechanical testing.[38] Mechanical integrity was ultimately found to correlate most with fiber alignment rather than proteoglycan content, highlighting the importance of structure over composition on the function of the disc.

Interestingly, diabetics are reported to have fasting blood glucose levels greater than 1250 mg/L, while hyperglycemia occurs around 1800 mg/L.[17] Taken together this evidence suggests that diabetes may not only aggravate the progression of DDD but may in fact play a detrimental role in the developing disc by impeding fiber formation, leading to a highly disorganized and ultimately mechanically inferior matrix. The purpose of this study, therefore, was to investigate the effect of hyperglycemia on the structure and mechanical function of developing IVDs. Using discs collected from mouse caudal spines, we assessed biochemical composition, fiber structure, and mechanical response to find that diabetic animals demonstrated noticeable detrimental changes to the disc as compared to nondiabetics.

2 | MATERIALS AND METHODS

2.1 | Sample preparation

Whole tails were harvested from 3- to 4-month-old female db/db (n = 8) and db/+ (n = 9) mice postmortem as described previously.[45] Caudal spines were then collected from the tails per existing protocol.[39,40]

2.2 | Diabetic characterization

Whole blood samples were collected at time of euthanasia following 6 hours of fasting, and fasting blood glucose levels were measured using a GLUCOCARD Vital blood glucose meter (ARKRAY, Edina, MN). A hemoglobin A1C (HbA1c) (Crystal Chem, Elk Grove Village, Illinois) assay was used to quantify glycemic control in these blood samples over the previous 2 to 3 months. Caudal discs were hydrolyzed in 12 N HCl for 3 hours to assay advanced glycation end product (AGE) content as previously described.[46] Fluorescence was measured against a quinine standard and normalized to hydroxyproline.

2.3 | Biochemical assays

Discs were extracted from the CA9/10 space and lyophilized for 48 hours prior to overnight digestion in a papain digest buffer. Biochemical content was then measured for each whole disc, NP and AF regions included, as previously described.[38,40,43] A Hoescht DNA assay,[47] modified 1,9-dimethylmethylene blue assay,[48] and hydroxyproline (hypro) assay[49] were used to measure DNA, sulfated glycosaminoglycan (s-GAG), and collagen content, respectively. These values were then normalized to wet weights, dry weights, and wet weight DNA content.

2.4 | Mechanical testing

Motion segments were collected from the CA7/8 disc space and adjacent vertebrae, then potted in poly(methyl methacrylate) (PMMA) (COE Tray Plastic, GC America, Alsip, IL) to prevent slippage during testing. To maintain hydration during mechanical tests, samples were wrapped in gauze soaked in PBS (Dulbecco's 1x PBS, Corning, New York) with added protease inhibitor (ThermoFisher Scientific, Waltham, Massachusetts). Segments were clamped at the potted ends and subjected to unconfined mechanical tests utilizing an ElectroForce (ELF) 5500 mechanical testing frame (TA Instruments, New Castle, Delaware) to determine biomechanical behavior.

Dynamic compressive responses were measured by applying a cyclic uniaxial loading protocol. A dynamic amplitude of 8% sinusoidal strain was imposed about the neutral position at 13 frequencies from 1 MHz to 1 Hz with 3 cycles per frequency. Time-dependent load response was measured at each of the frequencies. Following these tests, a uniaxial stress-relaxation protocol consisting of 10 incremental steps of 5% strain each up to 50% total strain was imposed on each sample. Time-dependent load response was measured at each of the steps.

Effective compressive moduli and hydraulic permeability were calculated for wild-type and diabetic samples using previously described poroelastic models and custom MATLAB codes, while equilibrium moduli and permeability were calculated using fiber-reinforced poroelastic models.[40,50,51]

2.5 | Histology

Motion segments from the aforementioned mechanical tests were prepared for histological assessment as previously described.[40,43,52–54] Segments were removed from the PMMA pots and cut closer to the endplates, then fixed in 10% buffered formalin for 48 hours prior to transfer to 70% ethanol. Following an overnight running water rinse, the segments were then decalcified in a solution consisting of 44%

formic acid and 20% sodium citrate. Based on previous studies,[40,54] samples were decalcified for 24 hours until bone was soft and flexible, then cut parallel to the sagittal plane and sliced to 5-μm thick sections. Sections were stained with either Safranin-O and a fast green counterstain for proteoglycan content, or picrosirius red for collagen network visualization. Safranin-O and picrosirius red stained sections were imaged using bright-field microscopy, and picrosirius red stained sections were additionally imaged with polarized light microscopy to qualitatively assess collagen alignment through birefringent intensity.

2.6 | Multiphoton microscopy

Motion segments were generated using the CA8/9 disc and adjacent vertebrae, then placed in 10% buffered formalin and transferred to 70% ethanol after 48 hours. Samples were sliced down the sagittal axis prior to imaging with a Zeiss LSM i-880 confocal microscope. 10×/0.45 C-Apochromat water immersion and 20×/0.75 Fluor DICII objectives were used as previously described,[36–38] and collagen fiber architecture was captured using second harmonic generation (SHG), with reflectance between 437 and 464 nm.

2.7 | Image processing and quantitative assessment

Safranin-O images of the whole disc were processed using ImageJ for quantitative staining assessment. Images were deconvolved in ImageJ and split into red, green, and blue color channels, after which intensity normalization and background subtraction were performed on the red. Depth of stain was subsequently calculated as the ratio of the number of pixels in the stained region over the number of pixels in the whole disc. The relative dimensions of the NP were also quantified by taking the ratio of pixels in the NP region and dividing by the pixels in the whole disc.
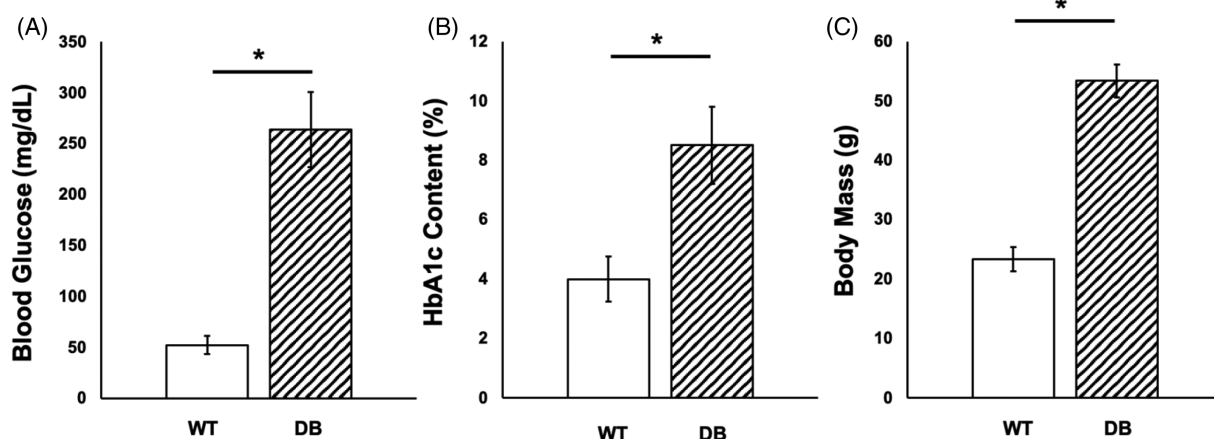

FIGURE 1 (A) Fasting blood glucose level, (B) percent HbA1c content, and (C) body mass measured for each group. Significant differences ($P < .05$) are indicated using (*) and bars. Error bars represent SD. (n = 8-9)

SHG images of the AF regions at 20× magnitude were processed using ImageJ as previously described[55] for quantitative fiber orientation assessment. Briefly, initial processing steps included intensity normalization, sharpening, background subtraction (sliding paraboloid/rolling ball), and smoothing. Images were then converted to 8-bit grayscale before a final noise removal (despeckle) step was applied. Fiber orientation in the AF region was determined for wild type and diabetic samples using the OrientationJ plugin.[56–58] The resulting orientation angle distributions from 0° to +90° were filtered to remove baseline noise and then normalized to total number of samples for each experimental group. The distributions were assumed to be symmetric and were mirrored to generate histograms for −90° to +90° orientations.

2.8 | Statistics

Dynamic stiffness was analyzed using a two-way analysis of variance with repeated measures, followed by Tukey's test for post-hoc analysis in R Studio. Differences in fiber orientation angle distributions were assessed using a χ^2 test for independence in R Studio. All other parameters were analyzed using a t test in MATLAB/Excel. Data are presented as mean ± SD, with significance determined at $P \le .05$.

3 | RESULTS

db/db mice are known to develop diabetes at 4 to 8 weeks of age, and as such had an average fasting blood glucose level of 263.6 ± 37.0 mg/dL (Figure 1A) and body mass of 53.34 ± 2.79 g (Figure 1C). db/+ mice meanwhile had an average fasting blood glucose level of 52.1 ± 8.8 mg/dL (Figure 1A) and body mass of 23.32 ± 2.03 g (Figure 1C). Diabetic animals also had an average HbA1c level of 8.5% ± 1.3% compared to wild-type mice at 4.0 ± 0.8% ($P < .05$), with levels of 6.5% and higher indicative of diabetes (Figure 1B). When normalized to wet weight, s-GAG content was higher in the diabetic discs, averaging at 34.0 ± 12.7 µg/mg compared to 27.8 ± 9.2 µg/mg in the wild type (Figure 2A, $P > .05$). Average collagen content as approximated from hydroxyproline concentration was also higher in the diabetic samples, with 300 ± 166 µg/mg present in the diabetic and 233 ± 134 µg/mg in the wild-type discs (Figure 2B, $P > .05$). The opposite trends were evident when s-GAG
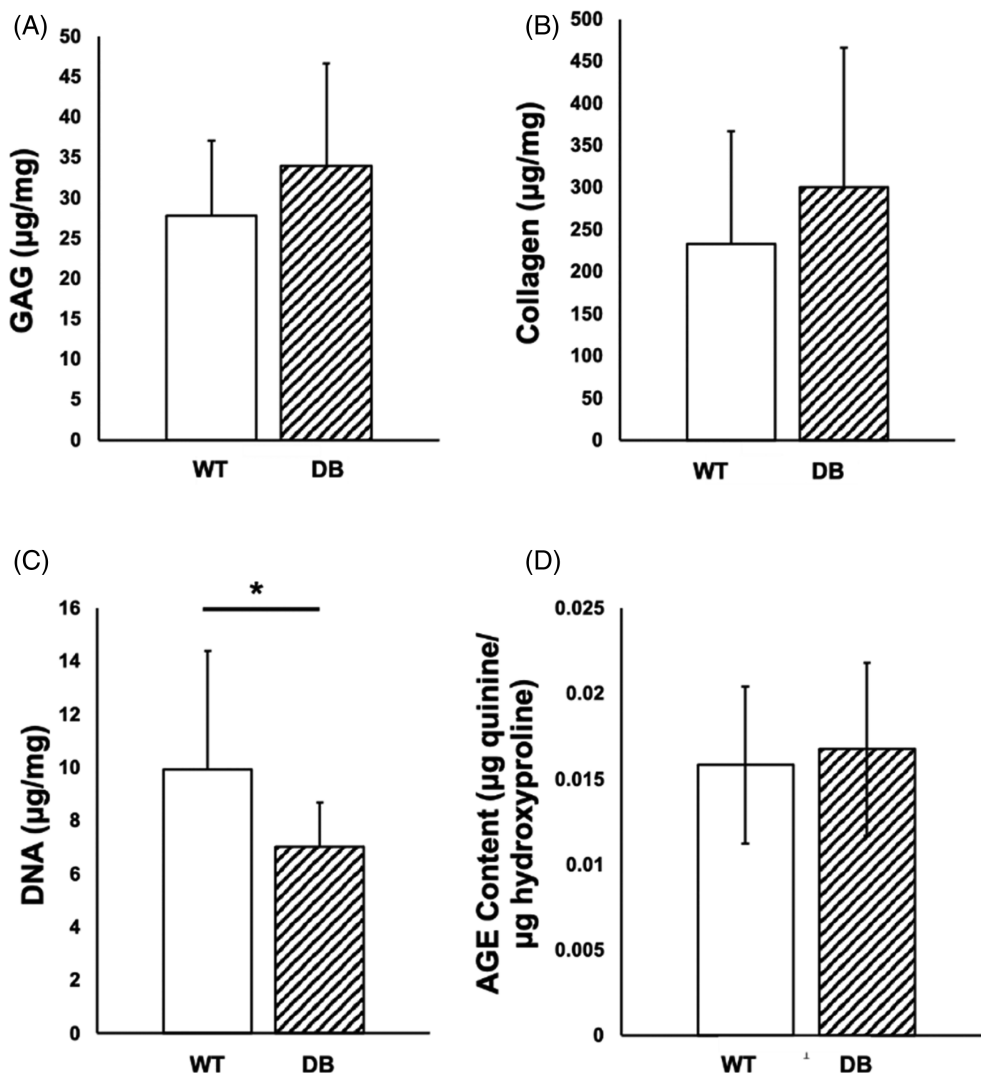

FIGURE 2 (A) Whole disc sulfated glycosaminoglycan (s-GAG) concentration, (B) whole disc collagen content, and (C) whole disc DNA content normalized to wet weight for each group. (D) Advanced glycation end products (AGE) content normalized to hydroxyproline for each group. Significant differences ($P < .05$) are indicated using (*) and bars. Error bars represent SD. (n = 8-9)

FIGURE 3 Representative histological images for Safranin-O staining of wild-type (top) and diabetic (bottom) discs of the (A) entire disc at 40× and (B) inner AF at 100× magnification. Significant differences (*P* < .05) are indicated using (*) and bars. Error bars represent SD while scale bars indicate 0.15 mm. (n = 5-6)
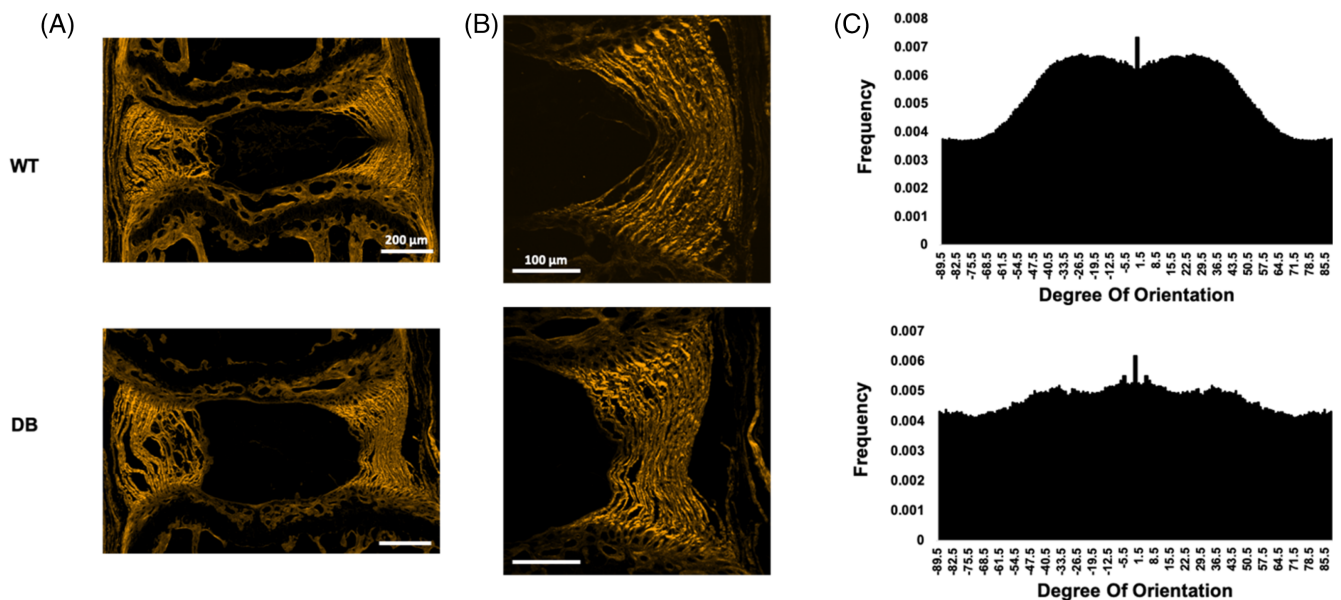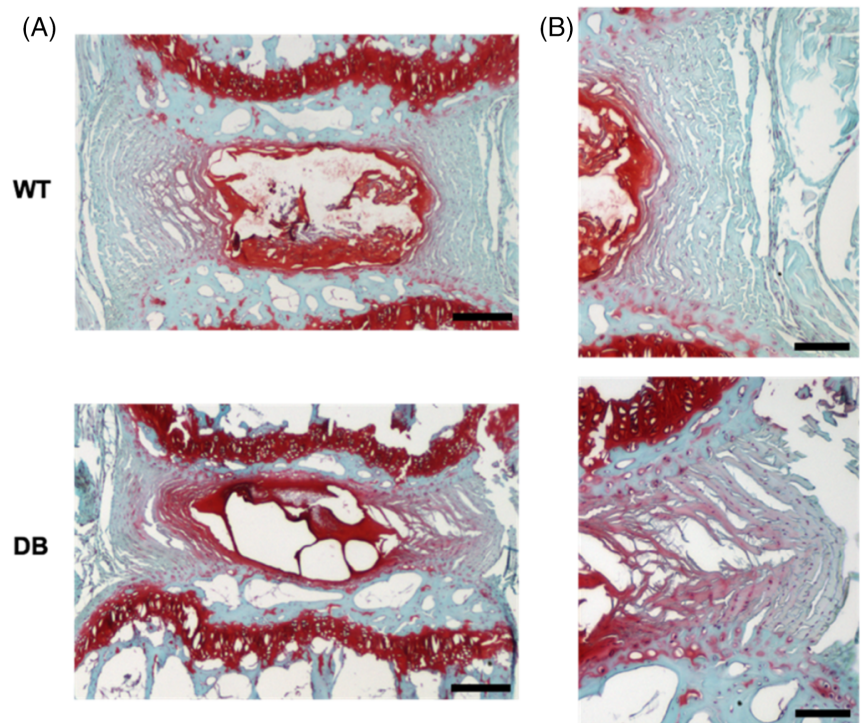

FIGURE 4 Representative second harmonic generation (SHG) images for wild-type (top) and diabetic (bottom) discs of the (A) entire disc and (B) inner annulus fibrosus (AF). (C) Normalized fiber orientation distributions for wild-type (top) and diabetic (bottom) discs. Scale bars indicate 200 (A) or 100 μm (B). (n = 6-7)

and collagen contents were normalized to dry weight (Figure S1A,B, *P* > .05), while normalization to DNA content displayed the same trends as wet weight normalization (Figure S1C,D, *P* ≤ .05). Wild-type discs showed significantly higher cell content than their diabetic counterparts (Figure 2C), with an average of 9.93 ± 4.46 μg/mg DNA content as compared to 7.02 ± 1.68 μg/mg in the diabetic discs (*P* < .05). No significant differences in AGE content were detected between

db/db (0.017 ± 0.005 μg quinine/μg hydroxyproline) and db/+ (0.016 ± 0.005 μg quinine/μg hydroxyproline) animals (Figure 2D, *P* > .05).

Gross histological images revealed morphological differences between the diabetic and wild-type IVDs. The NP regions in the diabetic discs appeared more oval than their wild-type counterparts, extending further into the disc with an irregular AF/NP boundary (Figure 3). They were also significantly larger, accounting for
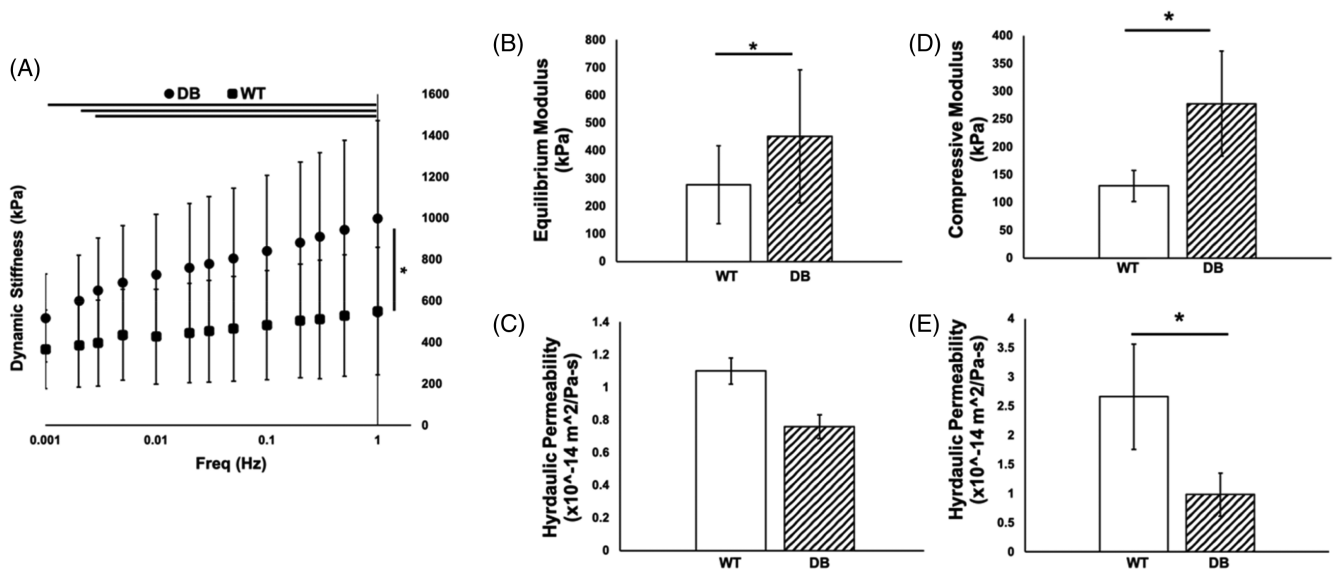
FIGURE 5 (A) Dynamic stiffness for each group over 13 frequencies. (B) Equilibrium modulus and (C) hydraulic permeability determined from stiffness and phase angle values following cyclic tests for each group. (D) Compressive modulus and (E) hydraulic permeability determined from stress/relaxation tests for each group. Significant differences ($P < .05$) are indicated using (*) and/or bars. Error bars represent SD. (n = 7-9)

approximately 41.8% of the whole disc area as compared to 35.1% in the wild-type discs (Figure S2A, $P < .05$). On average, there were no discernible differences in height:width ratios between the groups. Safranin-O staining for proteoglycan content also extended further past the NP boundary and into the inner AF for the diabetic discs as compared to the wild type, occupying 65.8% of the whole disc area in the former and 55.0% in the latter (Figure S2B, $P < .05$).

SHG microscopy also revealed subtle qualitative differences in the collagen fiber architecture at the inner AF between the two groups. Collagen fibers at the AF/NP border in diabetic discs appeared more disorganized and less aligned than in the wild-type samples, with larger gaps present between fiber bundles as well as bundles arranged at a wider variety of angles (Figure 4). The fiber bundles in wild-type IVDs were more tightly packed and oriented in a more parallel fashion. Quantitative analysis indicated two primary peaks in fiber orientation distribution for wild-type discs, centered around ±30° (Figure 4C). These peaks were also present for the diabetic discs, though the peaks were less prominent than in the wild type and the overall curve flatter to indicate a wider range of angles (Figure 4C). Approximately 10% and 13.3% of fibers lie within ±5° of the main peaks for the diabetic and wild-type discs, respectively. This trend of greater fiber organization in wild-type IVDs continues as the range of angles increases, with a ± 10° range yielding 20.0% and 26.4%; a ± 15° range yielding 29.9% and 39.2%; and a ± 20° range yielding 39.9% and 51.4%, for example. Of the aforementioned values, the groups were statistically distinct at the ±20° range alone ($\chi^2 = 121.89$, $P < .05$).

In order to assess mechanical response, samples were subjected to a two-part mechanical testing protocol consisting of (a) dynamic tension/compression about the neutral position and (b) compressive stress-relaxation. Both diabetic and wild-type discs demonstrated time- and frequency-dependent behavior in response to loading.

Following cyclic testing, average dynamic stiffness increased from 518 MPa at 1 MHz to 998 kPa at 1 Hz for the diabetic samples, while the wild-type demonstrated an average stiffness of 367 and 551 kPa at 1 MHz and 1 Hz, respectively (Figure 5A, $P < .05$). The dynamic stiffness data fit well to a poroelastic model (R^2 ranged from .84 to .99), enabling the calculation of an average equilibrium modulus of 232 kPa and hydraulic permeability of 1.1×10^{-14} m^2/Pa*s for the wild-type segments, while the diabetic averaged 451 kPa and 0.761×10^{-14} m^2/Pa*s in comparison (Figure 5B,C, $P < .05$).

Stress-relaxation data were also fit to a poroelastic model for calculation of material properties, with wild-type samples having an average compressive modulus of 130 kPa and hydraulic permeability of 2.71×10^{-14} m^2/Pa*s while their diabetic counterparts averaged 278 kPa and 0.981×10^{-14} m^2/Pa*s. (Figure 5D,E, $P < .05$).

4 | DISCUSSION

The objective of this study was to determine whether diabetes, a major risk factor for the development of DDD later in life, can generate significant degenerative changes to the developing IVD. Using caudal spines collected from 3- to 4-month-old db/db and db/+ mice, we quantified the structural and mechanical characteristics of the discs to determine if there were any major functional differences between diabetic and healthy animals. Our results indicate that increased levels of glucose appeared to impact the formation and deposition of fibers in the AF to result in an unaligned, disorganized matrix with biochemical and mechanical properties distinct from those present in physiologic or healthy levels of glucose.

In assessing ECM composition, we found that both bulk s-GAG and collagen content normalized to wet weight were higher in the

diabetic discs: the former demonstrated an average value approximately 22.1% larger than the wild type, the latter 29.0% larger (P > .05). Assessment of the microscopy and histology images yielded additional insight into the trends in proteoglycan content. In the healthy disc, proteoglycans were primarily contained in the NP, comprising 35% to 65% of the NP dry weight as opposed to 15% to 20% in the AF.[6,59–64] This is consistent with our wild-type samples, where the NP had a regular cross-section and was contained by a defined inner AF. In diabetic animals, however, the NP/AF boundary was ill-defined compared to the wild-type discs, with 6.7% greater Safranin-O staining, consistent with a higher proteoglycan content than in healthy animals.

Analysis of the collagen structure of AF showed significant differences between diabetic and wild-type mice. SHG microscopy revealed that the inner AF of the diabetic animals was structurally distinct from their wild-type counterparts, and appeared more disorganized, similar to what is seen in degeneration.[65] Compiling quantitative fiber orientation data supported this observation, showing that healthy fiber networks demonstrated clean peaks in orientation at ±30°, producing a bimodal distribution, while those in diabetic IVDs ranged across a broader distribution with less defined peaks. Taken together, these data point to a disruption in the structure of the disc that is associated with changes in biochemical components. Collectively, these data indicate that in diabetic animals, hyperglycemic levels of glucose were associated with an increase in proteoglycan content and a disruption in collagen organization.

Assessment of mechanical properties provided insight into the functional consequences of biochemical and structural changes in IVDs from diabetic animals. During cyclic testing, diabetic discs demonstrated almost twice the dynamic stiffness of their wild-type counterparts. When the dynamic stiffness and phase angle data from the cyclic tests were fit to a poroelastic model, the resulting equilibrium modulus and hydraulic permeability values observed the same trends: diabetic discs had approximately twice the moduli of their wild-type counterparts and half the permeability. Analysis of the stress-relaxation data had comparable differences between the experimental groups, with diabetic discs demonstrating an approximately twofold increase in compressive modulus over the wild-type as well as about half the hydraulic permeability. Both the wild-type and diabetic groups demonstrated dynamic moduli that were almost twice their stress-relaxation counterparts, likely explained by the differences between the tests. While stress-relaxation consists of solely compression, dynamic testing has an aspect of tension, and this incorporation may explain the twofold increase in dynamic modulus over stress-relaxation modulus. Despite these differences, the measured moduli are comparable to what has been seen in previous rodent in vivo studies. Rattail IVDs extracted from the caudal spine demonstrated an average compressive modulus of 238 kPa following the same stress-relaxation loading protocol used in this study.[40] Mouse caudal IVDs have been shown to range from 160 kPa to 2.48 MPa as compared to the 430 kPa to 3.65 MPa range seen in lumbar IVDs when exposed to a variety of testing regimes.[66] These results indicate that the diabetic discs were significantly stiffer than the wild-type and had a greater resistance to deformation as well as taking markedly longer to recover from deformation, as seen in previous studies.[33,67] Various groups have investigated the mechanisms governing the consequences of hyperglycemia on collagen matrix properties.[67–72] Matrix synthesis in collagen type I gels, for example, was found to be elevated in response to elevated levels of glucose, resulting in alterations to cell-matrix interactions, enhanced collagen fiber crosslinking and bundling, and ultimately matrix stiffening.[69–71] Diminished biomechanical behavior in IVDs specifically is attributed to increased disc tissue stiffness as a result of hyperglycemia.[68,72] As a result, the structural changes evident in the diabetic discs are likely contributing to their poor mechanical behavior. Specifically, the increased proteoglycan deposition and disrupted collagen structure at the NP/AF boundary may play a role in explaining mechanical discrepancies.

Numerous studies have determined a strong correlation between diabetes and DDD, as well as investigated the mechanisms by which diabetes and its comorbidities aggravate disc degeneration. As a consequence of long-term hyperglycemia the formation of AGEs is accelerated, the accumulation of which severely damages tissues on their own as well as stimulates the production of biologic mechanisms and other byproducts, such as oxidative species, which further degeneration.[73] For example activation of MMP-13, one of the main metalloproteinases associated with increased catabolism in DDD, is found to be stimulated by the presence of reactive oxygen species.[34,73–75] Hyperglycemia has also been found to promote the expression of factors which trigger apoptosis or senescence in discogenic cells, accelerating the progression of DDD in diabetic animals.[26,35] Additionally, the receptor for AGE (RAGE) has been implicated as a trigger for further inflammatory responses in the disc.[76–78] Increases in RAGE content via AGE accumulation, for example, have been shown to directly impact AF structure, resulting in increased collagen disruption and degeneration.[75,76] The structural changes brought about by early onset diabetes on developing discs, however, is less understood.

A striking feature of this model is the lack of AGE accumulation in these young animals. The results here suggest that the negative effects of hyperglycemia precede that of AGE accumulation. Since the formation of AGEs require sustained hyperglycemia, it is thus not surprising AGE accumulation is not elevated at this relatively short duration of hyperglycemia. Despite this lack of accumulation, there are clear changes to the ECM in the diabetic animals, notably significant deposition of proteoglycans in the inner AF. Interestingly, higher levels of AGEs present in diabetic animals have been shown to correlate with decreased proteoglycan content.[68,79,80] Our findings demonstrate that diabetic animals show distinct detrimental changes even at a young age and prior to AGE accumulation. These data indicate that the disease affects the manner in which the young disc is formed via an imbalance in its composition. Ultimately, this imbalance results in structural changes to the complex fiber architecture of the AF and the distinct AF/NP boundary which serves to contain the NP, consequences of an inferior matrix deposited by cells with altered metabolism. It has been established that the IVD's structure is fundamental to its function,[59,81,82] evident here where the disc's ability to resist

deformation is significantly impaired under diabetic conditions. Collectively our data suggest that while diabetes accelerates the progression of DDD later in life through the accumulation of AGEs, hyperglycemia associated with diabetes predisposes the disc to the disease through the presence of an ECM that is too rich in proteoglycans and deficient in fiber formation.

This deficiency in fiber formation is consistent with previous in vitro studies examining the effect of glucose media content on engineered fibrocartilage.[36–38] In general, many of the same trends observed in vitro in the development of TE-IVDs were reflected in this in vivo study. Wild-type mice in our cohort averaged a fasting blood glucose level of 52.1 mg/dL (or 521 mg/L), in line with the in vitro optimal glucose concentration (500 mg/L) that yielded both the highest degree of fiber alignment[36–38] and the highest effective stiffness.[38] db/db mice in our cohort meanwhile averaged a hyperglycemic blood glucose concentration of 263.6 mg/dL (2636 mg/L) when tested. This value lies between the two high glucose concentrations examined in vitro: 1000 mg/L (high physiologic) and 4500 mg/L (superphysiologic).[36–38] These higher glucose groups both saw substantial decreases in fiber alignment and effective stiffness as compared to the 500 mg/L group, indicating that glucose levels at the cusp of the physiologic limit will already affect the disc cell population and alter their metabolism, impacting their ability to effectively produce and maintain matrix. Collectively, these data point to the importance of monitoring blood glucose levels in vivo and in optimizing glucose concentration in culture media in experiments aimed at achieving robust collagen fiber formation in vitro.

One of the potential limitations of this study is that the db/db mutation in mice not only results in diabetes but also leads to additional phenotypical changes such as obesity. The db/+ mice in our cohort had an average body mass of 23.32 g while the db/db mice averaged a significantly higher body mass of 53.34 g (Figure S1B, $P < .05$). Obesity has been implicated as a major risk factor for DDD as well as a common comorbidity for diabetes[28,33,83,84] and as such the effects may be difficult to divorce from those arising as a result of diabetic hyperglycemia alone. However, as the discs were extracted from the tails of the animals, any loading effects resulting from obesity are likely minimal. We also note that while the mice used here are 3 to 4 months of age and are therefore young animals, not infants, db/db mice at this age are not yet fully grown.[85,86] As a result, the discs are likely still maturing along with the organism and may yet provide interesting insight into the mechanisms by which the diabetic disc arises. Additionally, compositional changes were assessed using bulk assays to determine total biochemical content. It appears, however, that abnormalities may arise in the diabetic disc from a more nuanced imbalance of factors. As DDD progresses, for example, there is a shift in collagen content in both the NP and AF, with the ratio of type I to type II collagen increasing in the NP and outer AF[65] as opposed to the healthy IVD. More precise assays, then, may yield a more complete understanding of the impact of diabetic hyperglycemia on the developing disc. To determine if these trends are also present in the developing disc, the presence of specific molecules—collagen types, for example—could be probed and identified through immunohistochemical analysis. Finally, due to the small size of murine caudal discs, NP and AF regions could not be separated for biochemical analysis. Given the histological assessments here indicated significant structural alterations to both the NP and inner AF sections of the diabetic disc, further analysis of the compositional changes associated with these observations could provide additional insight into the mechanisms responsible.

In conclusion, we found that diabetes and its associated hyperglycemia impact matrix formation in the IVD prior to the onset of DDD and independently of the accumulation of AGEs. Diabetic discs with superphysiological glucose levels displayed elevated proteoglycan content as compared to the wild-type mice; these trends corresponded to a greater degree of disorganization in the AF, ill-defined AF/NP boundaries, and impaired mechanical response to deformation. Ultimately, these observations indicate that diabetes impacts discogenic cells' ability to effectively produce and maintain matrix in development, altering the disc's basic structure and biomechanical function in such a manner that the disc is now primed for DDD later in life.

CONFLICT OF INTEREST

Dr L. J. B. is a co-founder of and holds equity in 3DBio Corp, and is a consultant for Fidia Farmaceutici, SpA, and Histogenics, Inc.

ORCID

Marianne Lintz https://orcid.org/0000-0002-3279-2167
Simon Y. Tang https://orcid.org/0000-0002-5570-3921

REFERENCES

1. Fatoye F, Gebrye T, Odeyemi I. Real-world incidence and prevalence of low back pain using routinely collected data. *Rheumatol Int*. 2019; *39*(4):619-626.
2. Rubin DI. Epidemiology and risk factors for spine pain. *Neurol Clin*. 2007;*25*(2):353-371.
3. Luoma K, Riihimäki H, Luukkonen R, Raininko R, Viikari-Juntura E, Lamminen A. Low back pain in relation to lumbar disc degeneration. *Spine*. 2000;*25*(4):487-492.
4. Urban JP, Roberts S. Degeneration of the intervertebral disc. *Arthritis Res Ther*. 2003;*5*(3):120-130.
5. Molinos M, Almeida CR, Caldeira J, Cunha C, Gonçalves RM, Barbosa MA. Inflammation in intervertebral disc degeneration and regeneration. *J R Soc Interface*. 2015;*12*(108):20150429.
6. Buckwalter JA. Aging and degeneration of the human intervertebral disc. *Spine*. 1995;*20*(11):1307-1314.

7. Lyons G, Eisenstein SM, Sweet MB. Biochemical changes in intervertebral disc degeneration. *Biochim Biophys Acta*. 1981;*673*(4):443-453.

8. Freemont AJ, Watkins A, Le Maitre C, Jeziorska M, Hoyland JA. Current understanding of cellular and molecular events in intervertebral disc degeneration: implications for therapy. *J Pathol*. 2002;*196*(4):374-379.

9. Liu J, Roughley PJ, Mort JS. Identification of human intervertebral disc stromelysin and its involvement in matrix degradation. *J Orthop Res*. 1991;*9*(4):568-575.

10. Liu MH, Sun C, Yao Y, et al. Matrix stiffness promotes cartilage endplate chondrocyte calcification in disc degeneration via miR-20a targeting ANKH expression. *Sci Rep*. 2016;*6*:25401.

11. Kanemoto M, Hukuda S, Komiya Y, Katsuura A, Nishioka J. Immunohistochemical study of matrix metalloproteinase-3 and tissue inhibitor of metalloproteinase-1 human intervertebral discs. *Spine*. 1996;*21*(1):1-8.

12. Nemoto O, Yamagishi M, Yamada H, Kikuchi T, Takaishi H. Matrix metalloproteinase-3 production by human degenerated intervertebral disc. *J Spinal Disord*. 1997;*10*(6):493-498.

13. Kang JD, Georgescu HI, McIntyre-Larkin L, Stefanovic-Racic M, Evans CH. Herniated cervical intervertebral discs spontaneously produce matrix metalloproteinases, nitric oxide, interleukin-6, and prostaglandin E2. *Spine*. 1995;*20*(22):2373-2378.

14. Kang JD, Georgescu HI, McIntyre-Larkin L, Stefanovic-Racic M, Donaldson WF 3rd, Evans CH. Herniated lumbar intervertebral discs spontaneously produce matrix metalloproteinases, nitric oxide, interleukin-6, and prostaglandin E2. *Spine*. 1996;*21*(3):271-277.

15. Guthrie RA, Guthrie DW. Pathophysiology of diabetes mellitus. *Crit Care Nurs Q*. 2004;*27*(2):113-125.

16. Schmidt AM. Highlighting diabetes mellitus: the epidemic continues. *Arterioscler Thromb Vasc Biol*. 2018;*38*(1):e1-e8.

17. American Diabetes Association. Classification and diagnosis of diabetes. *Diabetes Care*. 2015;*38*(suppl 1):S8-S16.

18. Lascar N, Brown J, Pattison H, Barnett AH, Bailey CJ, Bellary S. Type 2 diabetes in adolescents and young adults. *Lancet Diabetes Endocrinol*. 2018;*6*(1):69-80.

19. International Diabetes Federation. *IDF Diabetes Atlas*. 9th ed. Brussels, Belgium: International Diabetes Federation; 2019.

20. Gaiz A, Mosawy S, Colson N, Singh I. Thrombotic and cardiovascular risks in type two diabetes; role of platelet hyperactivity. *Biomed Pharmacother*. 2017;*94*:679-686.

21. Cole JB, Florez JC. Genetics of diabetes mellitus and diabetes complications. *Nat Rev Nephrol*. 2020;*16*(7):377-390.

22. Zheng Y, Ley SH, Hu FB. Global aetiology and epidemiology of type 2 diabetes mellitus and its complications. *Nat Rev Endocrinol*. 2018;*14*(2):88-98.

23. Cannata F, Vadalà G, Ambrosio L, et al. Intervertebral disc degeneration: a focus on obesity and type 2 diabetes. *Diabetes Metab Res Rev*. 2020;*36*(1):e3224.

24. Alpantaki K, Kampouroglou A, Koutserimpas C, Effraimidis G, Hadjipavlou A. Diabetes mellitus as a risk factor for intervertebral disc degeneration: a critical review. *Eur Spine J*. 2019;*28*(9):2129-2144.

25. Li X, Liu X, Wang Y, et al. Intervertebral disc degeneration in mice with type II diabetes induced by leptin receptor deficiency. *BMC Musculoskelet Disord*. 2020;*21*(1):77.

26. Zhang Y, Proenca R, Maffei M, Barone M, Leopold L, Friedman JM. Positional cloning of the mouse obese gene and its human homologue. *Nature*. 1994;*372*(6505):425-432.

27. Kivimäki M, Virtanen M, Kawachi I, et al. Long working hours, socioeconomic status, and the risk of incident type 2 diabetes: a meta-analysis of published and unpublished data from 222 120 individuals. *Lancet Diabetes Endocrinol*. 2015;*3*(1):27-34.

28. Jakoi AM, Pannu G, D'Oro A, et al. The clinical correlations between diabetes, cigarette smoking and obesity on intervertebral degenerative disc disease of the lumbar spine. *Asian Spine J*. 2017;*11*(3):337-347.

29. Sakellaridis N. The influence of diabetes mellitus on lumbar intervertebral disk herniation. *Surg Neurol*. 2006;*66*(2):152-154.

30. Anekstein Y, Smorgick Y, Lotan R, et al. Diabetes mellitus as a risk factor for the development of lumbar spinal stenosis. *Isr Med Assoc J*. 2010;*12*(1):16-20.

31. Teraguchi M, Yoshimura N, Hashizume H, et al. Prevalence and distribution of intervertebral disc degeneration over the entire spine in a population-based cohort: the Wakayama Spine Study. *Osteoarthr Cartil*. 2014;*22*(1):104-110.

32. Mobbs RJ, Newcombe RL, Chandran KN. Lumbar discectomy and the diabetic patient: incidence and outcome. *J Clin Neurosci*. 2001;*8*(1):10-13.

33. Mahmoud M, Kokozidou M, Auffarth A, Schulze-Tanzil G. The relationship between diabetes mellitus type II and intervertebral disc degeneration in diabetic rodent models: a systematic and comprehensive review. *Cell*. 2020;*9*(10):2208.

34. Wang J, Hu J, Chen X, et al. BRD4 inhibition regulates MAPK, NF-κB signals, and autophagy to suppress MMP-13 expression in diabetic intervertebral disc degeneration. *FASEB J*. 2019;*33*(10):11555-11566.

35. Jiang L, Zhang X, Zheng X, et al. Apoptosis, senescence, and autophagy in rat nucleus pulposus cells: implications for diabetic intervertebral disc degeneration. *J Orthop Res*. 2013;*31*(5):692-702.

36. McCorry MC, Kim J, Springer NL, Sandy J, Plaas A, Bonassar LJ. Regulation of proteoglycan production by varying glucose concentrations controls fiber formation in tissue engineered menisci. *Acta Biomater*. 2019;*100*:173-183.

37. Kim J, Boys AJ, Estroff LA, Bonassar LJ. Combining TGF-β1 and mechanical anchoring to enhance collagen fiber formation and alignment in tissue-engineered menisci. *ACS Biomater Sci Eng*. 2021;*7*(4):1608-1620.

38. Lintz M. Tissue engineering strategies for total disc replacement: structure and mechanical function of the Intervertebral disc. Dissertation. New York: Cornell University; 2021.

39. Bowles RD, Williams RM, Zipfel WR, Bonassar LJ. Self-assembly of aligned tissue-engineered annulus fibrosus and intervertebral disc composite via collagen gel contraction. *Tissue Eng Part A*. 2010;*16*(4):1339-1348.

40. Bowles RD, Gebhard HH, Härtl R, Bonassar LJ. Tissue-engineered intervertebral discs produce new matrix, maintain disc height, and restore biomechanical function to the rodent spine. *Proc Natl Acad Sci U S A*. 2011;*108*(32):13106-13111.

41. Bowles RD, Gebhard HH, Dyke JP, et al. Image-based tissue engineering of a total intervertebral disc implant for restoration of function to the rat lumbar spine. *NMR Biomed*. 2012;*25*(3):443-451.

42. Hudson KD, Mozia RI, Bonassar LJ. Dose-dependent response of tissue-engineered intervertebral discs to dynamic unconfined compressive loading. *Tissue Eng Part A*. 2015;*21*(3–4):564-572.

43. Moriguchi Y, Mojica-Santiago J, Grunert P, et al. Total disc replacement using tissue-engineered intervertebral discs in the canine cervical spine. *PLoS One*. 2017;*12*(10):e0185716.

44. Mojica-Santiago JA, Lang GM, Navarro-Ramirez R, Hussain I, Härtl R, Bonassar LJ. Resorbable plating system stabilizes tissue-engineered intervertebral discs implanted ex vivo in canine cervical spines. *JOR Spine*. 2018;*1*(3):e1031.

45. Walk RE, Tang SY. In vivo contrast-enhanced microCT for the monitoring of mouse thoracic, lumbar, and coccygeal intervertebral discs. *JOR Spine*. 2019;*2*(2):e1058.

46. Tang SY, Zeenath U, Vashishth D. Effects of non-enzymatic glycation on cancellous bone fragility. *Bone*. 2007;*40*(4):1144-1151.

47. Kim YJ, Sah RL, Doong JY, Grodzinsky AJ. Fluorometric assay of DNA in cartilage explants using Hoechst 33258. *Anal Biochem*. 1988;*174*(1):168-176.

48. Enobakhare BO, Bader DL, Lee DA. Quantification of sulfated glycosaminoglycans in chondrocyte/alginate cultures, by use of 1,9-dimethylmethylene blue. *Anal Biochem*. 1996;*243*(1):189-191.

49. Neuman R, Logan M. The determination of hydroxyproline. *J Biol Chem*. 1950;*184*(1):299-306.

50. Frank EH, Grodzinsky AJ. Cartilage electromechanics—II. A continuum model of cartilage electrokinetics and correlation with experiments. *J Biomech*. 1987;*20*(6):629-639.

51. Kim YJ, Bonassar LJ, Grodzinsky AJ. The role of cartilage streaming potential, fluid flow and pressure in the stimulation of chondrocyte biosynthesis during dynamic compression. *J Biomech*. 1995;*28*(9): 1055-1066.

52. Sloan SR Jr, Wipplinger C, Kirnaz S, et al. Combined nucleus pulposus augmentation and annulus fibrosus repair prevents acute intervertebral disc degeneration after discectomy. *Sci Transl Med*. 2020; *12*(534):eaay2380.

53. Hussain I, Sloan SR, Wipplinger C, et al. Mesenchymal stem cell-seeded high-density collagen gel for annular repair: 6-week results from in vivo sheep models. *Neurosurgery*. 2019;*85*(2):E350-E359.

54. Boys AJ, Zhou H, Harrod JB, McCorry MC, Estroff LA, Bonassar LJ. Top-down fabrication of spatially controlled mineral-gradient scaffolds for interfacial tissue engineering. *ACS Biomater Sci Eng*. 2019; *5*(6):2988-2997.

55. Morrill EE, Tulepbergenov AN, Stender CJ, Lamichhane R, Brown RJ, Lujan TJ. A validated software application to measure fiber organization in soft tissue. *Biomech Model Mechanobiol*. 2016;*15*(6):1467-1478.

56. Püspöki Z, Storath M, Sage D, Unser M. Transforms and operators for directional bioimage analysis: a survey. *Adv Anat Embryol Cell Biol*. 2016;*219*:69-93.

57. Rezakhaniha R, Agianniotis A, Schrauwen JT, et al. Experimental investigation of collagen waviness and orientation in the arterial adventitia using confocal laser scanning microscopy. *Biomech Model Mechanobiol*. 2012;*11*(3–4):461-473.

58. Fonck E, Feigl GG, Fasel J, et al. Effect of aging on elastin functionality in human cerebral arteries. *Stroke*. 2009;*40*(7):2552-2556.

59. Newell N, Little JP, Christou A, Adams MA, Adam CJ, Masouros SD. Biomechanics of the human intervertebral disc: a review of testing techniques and results. *J Mech Behav Biomed Mater*. 2017;*69*:420-434.

60. Dickson IR, Happey F, Pearson CH, Naylor A, Turner RL. Variations in the protein components of human intervertebral disk with age. *Nature*. 1967;*215*(5096):52-53.

61. Iatridis JC, Weidenbaum M, Setton LA, Mow VC. Is the nucleus pulposus a solid or a fluid? Mechanical behaviors of the nucleus pulposus of the human intervertebral disc. *Spine*. 1996;*21*(10):1174-1184.

62. McDevitt CA. Proteoglycans of the intervertebral disc. *The Biology of the Intervertebral Disc*. Boca Raton, FL; CRC Press; 1988.

63. Eyre DR, Muir H. Types I and II collagens in intervertebral disc. Interchanging radial distributions in annulus fibrosus. *Biochem J*. 1976; *157*(1):267-270.

64. Eyre DR. Collagens of the disc. *The Biology of the Intervertebral Disc*. Boca Raton, FL: CRC Press; 1988.

65. Dowdell J, Erwin M, Choma T, Vaccaro A, Iatridis J, Cho SK. Intervertebral disk degeneration and repair. *Neurosurgery*. 2017;*80*(3S): S46-S54.

66. Sarver JJ, Elliott DM. Mechanical differences between lumbar and tail discs in the mouse. *J Orthop Res*. 2005;*23*(1):150-155.

67. Krishnamoorthy D, Hoy RC, Natelson DM, et al. Dietary advanced glycation end-product consumption leads to mechanical stiffening of murine intervertebral discs. *Dis Model Mech*. 2018;*11*(12): dmm036012.

68. Fields AJ, Berg-Johansen B, Metz LN, et al. Alterations in intervertebral disc composition, matrix homeostasis and biomechanical behavior in the UCD-T2DM rat model of type 2 diabetes. *J Orthop Res*. 2015;*33*(5):738-746.

69. Dandia H, Makkad K, Tayalia P. Glycated collagen—a 3D matrix system to study pathological cell behavior. *Biomater Sci*. 2019;*7*(8):3480-3488.

70. McCarthy AD, Etcheverry SB, Bruzzone L, Lettieri G, Barrio DA, Cortizo AM. Non-enzymatic glycosylation of a type I collagen matrix: effects on osteoblastic development and oxidative stress. *BMC Cell Biol*. 2001;*2*:16.

71. Kent MJ, Light ND, Bailey AJ. Evidence for glucose-mediated covalent cross-linking of collagen after glycosylation in vitro. *Biochem J*. 1985;*225*(3):745-752.

72. Wagner DR, Reiser KM, Lotz JC. Glycation increases human annulus fibrosus stiffness in both experimental measurements and theoretical predictions. *J Biomech*. 2006;*39*(6):1021-1029.

73. Waldron AL, Schroder PA, Bourgon KL, et al. Oxidative stress-dependent MMP-13 activity underlies glucose neurotoxicity. *J Diabetes Complicat*. 2018;*32*(3):249-257.

74. Chen YJ, Chan DC, Lan KC, et al. PPARγ is involved in the hyperglycemia-induced inflammatory responses and collagen degradation in human chondrocytes and diabetic mouse cartilages. *J Orthop Res*. 2015;*33*(3):373-381.

75. Chen YJ, Chan DC, Chiang CK, et al. Advanced glycation end-products induced VEGF production and inflammatory responses in human synoviocytes via RAGE-NF-κB pathway activation. *J Orthop Res*. 2016;*34*(5):791-800.

76. Hoy RC, D'Erminio DN, Krishnamoorthy D, et al. Advanced glycation end products cause RAGE-dependent annulus fibrosus collagen disruption and loss identified using in situ second harmonic generation imaging in mice intervertebral disk in vivo and in organ culture models. *JOR Spine*. 2020;*3*(4):e1126.

77. Illien-Jünger S, Palacio-Mancheno P, Kindschuh WF, et al. Dietary advanced glycation end products have sex- and age-dependent effects on vertebral bone microstructure and mechanical function in mice. *J Bone Miner Res*. 2018;*33*(3):437-448.

78. Nerlich AG, Bachmeier BE, Schleicher E, Rohrbach H, Paesold G, Boos N. Immunomorphological analysis of RAGE receptor expression and NF-kappaB activation in tissue samples from normal and degenerated intervertebral discs of various ages. *Ann N Y Acad Sci*. 2007;*1096*:239-248.

79. Yokosuka K, Park JS, Jimbo K, et al. Advanced glycation end-products downregulating intervertebral disc cell production of proteoglycans in vitro. *J Neurosurg Spine*. 2006;*5*(4):324-329.

80. Illien-Jünger S, Grosjean F, Laudier DM, Vlassara H, Striker GE, Iatridis JC. Combined anti-inflammatory and anti-AGE drug treatments have a protective effect on intervertebral discs in mice with diabetes. *PLoS One*. 2013;*8*(5):e64302.

81. Humzah MD, Soames RW. Human intervertebral disc: structure and function. *Anat Rec*. 1988;*220*(4):337-356.

82. Adams MA, Roughley PJ. What is intervertebral disc degeneration, and what causes it? *Spine*. 2006;*31*(18):2151-2161.

83. Coppock JA, Danyluk ST, Englander ZA, Spritzer CE, Goode AP, DeFrate LE. Increasing BMI increases lumbar intervertebral disc deformation following a treadmill walking stress test. *J Biomech*. 2021;*121*:110392.

84. Parenteau CS, Lau EC, Campbell IC, Courtney A. Prevalence of spine degeneration diagnosis by type, age, gender, and obesity using Medicare data. *Sci Rep*. 2021;*11*(1):5389.

85. Srinivasan K, Ramarao P. Animal models in type 2 diabetes research: an overview. *Indian J Med Res*. 2007;*125*(3):451-472.

86. Lindström P. The physiology of obese-hyperglycemic mice [ob/ob mice]. *Sci World J*. 2007;*7*:666-685.

SUPPORTING INFORMATION

Additional supporting information may be found in the online version of the article at the publisher's website.